

Abstract

One of the most challenging tasks for chemical transport models (CTMs) is the prediction of the formation and partitioning of the major semi-volatile inorganic aerosol components (nitrate, chloride, ammonium) between the gas and particulate phases. In this work the PMCAMx-2008 CTM, which includes the recently developed aerosol thermodynamic model ISORROPIA-II, is applied in the Mexico City Metropolitan Area in order to simulate the formation of the major inorganic aerosol components. The main sources of SO₂ (such as the Miguel Hidalgo Refinery and the Francisco Perez Rios Power Plant) in the Mexico City Metropolitan Area (MCMA) are located in Tula, resulting in high predicted PM₁ sulfate concentrations (over 25 μg m⁻³) in that area. The average predicted PM₁ nitrate concentrations are up to 3 μg m⁻³ (with maxima up to 11 μg m⁻³) in and around the urban center, mostly produced from local photochemistry. The presence of calcium coming from the Tolteca area (7 μg m⁻³) as well as the rest of the mineral cations (1 μg m⁻³ potassium, 1 μg m⁻³ magnesium, 2 μg m⁻³ sodium, and 3 μg m⁻³ calcium) from the Texcoco Lake resulted in the formation of a significant amount of aerosol nitrate in the coarse mode with concentrations up to 3 μg m⁻³ over these areas. PM₁₋₁₀ chloride is also high and its concentration exceeds 2 μg m⁻³ in Texcoco Lake. PM₁ ammonium concentrations peak at the center of Mexico City (2 μg m⁻³) and the Tula vicinity (2.5 μg m⁻³). The performance of the model for the major inorganic PM components (sulfate, ammonium, nitrate, chloride, sodium, calcium, and magnesium) is encouraging. At T0, the average measured values of PM₁ sulfate, nitrate, ammonium, and chloride are 3.6 μg m⁻³, 3.6 μg m⁻³, 2.1 μg m⁻³, and 0.35 μg m⁻³ respectively. The corresponding predicted values are 3.7 μg m⁻³, 2.8 μg m⁻³, 1.7 μg m⁻³, and 0.25 μg m⁻³. Additional improvements are possible by (i) using a day-dependent emission inventory, (ii) improving the performance of the model regarding the oxidant levels, and (iii) revising the emissions and the chemical composition of the fugitive dust. Sensitivity tests indicate that sulfate concentration in Tula decreases by up to 0.5 μg m⁻³ after a 50% reduction of SO₂ emissions while it can increase by up to 0.3 μg m⁻³ when NO_x emis-

Formation of semivolatile inorganic aerosols

V. A. Karydis et al.

Title Page

Abstract

Introduction

Conclusions

References

Tables

Figures

◀

▶

◀

▶

Back

Close

Full Screen / Esc

Printer-friendly Version

Interactive Discussion



sions are reduced by 50 %. Nitrate concentration decreases by up to $1 \mu\text{g m}^{-3}$ after the 50 % reduction of NO_x or NH_3 emissions. Ammonium concentration decreases by up to $1 \mu\text{g m}^{-3}$, $0.3 \mu\text{g m}^{-3}$, and $0.1 \mu\text{g m}^{-3}$ after the 50 % reduction of NH_3 , NO_x , and SO_2 emissions respectively.

1 Introduction

The rapid growth of megacities has led to serious urban air pollution problems in many developing countries. For example, Mexico City is the largest metropolitan area in North America with a population of 20 million. This megacity is experiencing high aerosol pollutant concentrations from a combination of high anthropogenic emissions, weak winds and intense sunshine (Molina and Molina, 2002). A large part of the $\text{PM}_{2.5}$ mass ($\sim 55\%$) is inorganic, with sulfates, nitrates, ammonium, sodium and chloride being the dominant species. Nitrate can be found in both fine (particles with diameters less than $1 \mu\text{m}$) and coarse (particles with diameters more than $1 \mu\text{m}$) modes. Sodium, chloride and the crustal components are mainly found in the coarse mode while ammonium and sulfate are usually in the fine mode (Seinfeld and Pandis, 2006). Mineral dust also plays an important role in Mexico City atmosphere. Analysis of model and observational data in the Mexico City area during the MILAGRO (Megacity Initiative: Local and Global Research Observations) field experiment suggests that the large area of coastal dry lands to the northeast of Mexico City is an important source of dust particles for the entire MCMA. During dust aerosol events, observed from 16 to 20 March 2006, dust aerosol mass accounts for about 70 % of the total PM_{10} aerosol mass concentrations, with a strong diurnal variation (Ying et al., 2011). These results also suggest that dust aerosols have important effects on actinic fluxes and therefore photochemistry in the MCMA.

The MILAGRO (<http://www.eol.ucar.edu/projects/milagro/>) field campaign was designed to follow the urban plume originating in Mexico City in order to study the evolution of the properties of trace gases and aerosols as they drifted downwind from a

Formation of semivolatile inorganic aerosols

V. A. Karydis et al.

Title Page

Abstract

Introduction

Conclusions

References

Tables

Figures

◀

▶

◀

▶

Back

Close

Full Screen / Esc

Printer-friendly Version

Interactive Discussion



megacity. The study was conducted over multiple scales, ranging from ground-based investigations centered in the Mexico City metropolitan area to aircraft sampling over distances of hundreds of kilometres (Molina et al., 2010). A major component of the MILAGRO campaign was the use of the observed data to evaluate the performance of three dimensional chemical transport models and then use them for the design of emission control strategies.

Several atmospheric models have been developed based on thermodynamic equilibrium principles to predict inorganic atmospheric aerosol behavior. These include: EQUIL (Bassett and Seinfeld, 1983), MARS (Saxena et al., 1986), SEQUILIB (Pili- nis and Seinfeld, 1987), AIM (Wexler and Seinfeld, 1991), SCAPE (Kim et al., 1993a, b), SCAPE2 (Kim and Seinfeld, 1995; Meng et al., 1995), EQUISOLV (Jacobson et al., 1996), AIM2 (Clegg et al., 1998a, b), ISORROPIA (Nenes et al., 1998), GFEMM (Ansari and Pandis, 1999a) and EQUISOLV II (Jacobson, 1999). These models have been used in determining emissions control strategies (Watson et al., 1994; Ansari and Pandis, 1998; Kumar et al., 1998), in analyzing ambient measurements (Ansari and Pandis, 1999b, 2000) and directly in large-scale chemical transport models (Pilin- is and Seinfeld, 1988; Lurmann et al., 1997; Jacobson et al., 1996; Jacobson, 1997a, b; Meng et al., 1998; Nenes et al., 1999). Several studies have been performed comparing field measurements of inorganic gaseous species and their particulate forms versus theory (Tanner, 1982; Hildemann et al., 1984). Tanner (1982) compared theo- retical equilibrium calculations versus observed partial pressure products of nitric acid and ammonia under conditions present on Long Island, New York and reported a gen- eral agreement although some differences were found. Hildemann et al. (1984) per- formed a similar comparison between equilibrium-based calculations and observed partial pressure products of nitric acid and ammonia and their particulate forms at dif- ferent locations in Southern California. At inland sites like Anaheim and Rubidoux, an overall agreement was reported although some discrepancies were found at Long Beach. Although comparison of calculated and observed partial pressure products of NH_3 and HNO_3 can provide an alternative way of testing an atmospheric equilibrium

Formation of semivolatile inorganic aerosols

V. A. Karydis et al.

Title Page

Abstract

Introduction

Conclusions

References

Tables

Figures

◀

▶

◀

▶

Back

Close

Full Screen / Esc

Printer-friendly Version

Interactive Discussion



**Formation of
semivolatile
inorganic aerosols**V. A. Karydis et al.

[Title Page](#)[Abstract](#)[Introduction](#)[Conclusions](#)[References](#)[Tables](#)[Figures](#)[⏪](#)[⏩](#)[◀](#)[▶](#)[Back](#)[Close](#)[Full Screen / Esc](#)[Printer-friendly Version](#)[Interactive Discussion](#)

model, interpretations of these comparisons are often difficult, especially in evaluating the ability of these models to reproduce particulate nitrate concentrations. An analysis of model performance against measurements has been performed by Russell et al. (1988), Pilinis and Seinfeld (1987), Wexler and Seinfeld (1991), Kumar et al. (1998), Ansari and Pandis (1999b), and Zhang et al. (2000, 2002). The first multicomponent particulate matter atmospheric models were developed and applied in California. An Eulerian model was used to describe the transport and formation of pollutants in the south California air basin by Russell et al. (1988). A three dimensional Eulerian CTM simulating the major inorganic and organic PM components and their size distribution was developed by Pilinis and Seinfeld (1987). Both of these initial models were evaluated in Los Angeles for the 30–31 August 1982 smog episode. Wexler and Seinfeld (1991) developed a model of the temporal composition of atmospheric aerosol particles based on their transport and thermodynamic properties. Components of the model were tested against measurements of activity coefficients in single- and multi-component aqueous solutions and general agreement was found. Kumar et al. (1998) compared the performance of several equilibrium models against measurements taken during the 1995 Integrated Monitoring Study (Chow and Egami, 1997). In these cases, the mean predictions of PM_{10} nitrate and ammonium agreed within 20–30 % of the corresponding measurements. Ansari and Pandis (1999b) compared the performance of SEQUILIB, SCAPE2, ISORROPIA and GFEMN and found a general agreement in predictions for particulate nitrate and total inorganic particulate matter (PM) over a broad range of temperature, relative humidity (RH) and composition. However, they found significant differences in predictions for particulate water concentrations. Against measurements from the Southern California Air Quality Study (SCAQS, Lawson, 1990), all models qualitatively reproduced but generally underpredicted $PM_{2.5}$ nitrate concentrations (mean normalized biases less than 30 %). Zhang et al. (2000) compared the performance of SCAPE2, AIM2 and EQUISOLV II and found similar results in model predictions for total PM over a broad range of RH and composition although some differences over species concentration and RH regimes were reported. Data obtained

during the 1999 Atlanta Supersite Experiment was used to test the validity of the assumption of thermodynamic equilibrium between the inorganic fine particulate matters and their gas-phase precursors (Zhang et al., 2002). The equilibrium gas-phase concentrations were calculated using the ISORROPIA model which was predicting the equilibrium $\text{NH}_3(\text{g})$ generally less than its observed concentration and the $\text{HNO}_3(\text{g})$ generally greater than the observed concentration.

Several photochemical modeling studies have been carried out in the MCMA. Among them, Zhang et al. (2009) and Tie et al. (2009) used the fully coupled WRF/CHEM (Weather Research and Forecasting – Chemistry) model to study the origin and evolution of the gaseous criteria pollutants (CO , O_3 , NO_x , NO_y) during the MILAGRO and MIRAGE-Mex field campaigns respectively. However, there have been rather limited efforts to predict particle concentrations in Mexico City by using three-dimensional chemical transport models (CTMs). Tsimpidi et al. (2010, 2011) applied PMCAMx-2008 simulating the organic aerosol formation during the MCMA-2003 and MILAGRO-2006 campaigns by using the volatility basis set framework assuming that both primary and secondary organic components are semi-volatile and photochemically reactive. Hodzic et al. (2009, 2010) used CHIMERE to study the contribution of biogenic organic compounds and semivolatile primary organic compounds to the formation of secondary organic aerosols in Mexico City during the MILAGRO field project. Li et al. (2011) simulated the organic aerosol concentrations in Mexico City using the WRF/CHEM model. Even fewer studies have focused on the formation of the inorganic aerosols in Mexico City. Fountoukis et al. (2009) coupled fast measurements of aerosol and gas-phase constituents with the ISORROPIA-II thermodynamic model to study the partitioning of semivolatile inorganic species and phase state of Mexico City aerosol during the MILAGRO 2006 campaign. Karydis et al. (2010) introduced the ISORROPIA-II model into PMCAMx-2008 and applied it to the MCMA in order to simulate the chemical composition and mass of the major PM_{10} (fine) and PM_{1-10} (coarse) inorganic components and determine the effect of mineral dust on their formation during a week of April 2003. However, major sources which are located approximately 100 km north-northwest of

Formation of semivolatile inorganic aerosols

V. A. Karydis et al.

Title Page

Abstract

Introduction

Conclusions

References

Tables

Figures

◀

▶

◀

▶

Back

Close

Full Screen / Esc

Printer-friendly Version

Interactive Discussion



Mexico City center (in the Tula industrial area) were not included in the model domain resulting in a small underprediction of all semivolatile inorganic components. The Karydis et al. (2010) study was also limited by the availability of measurements in Mexico City and the surrounding area (there was just one site with continuous PM composition measurements).

The present study adds to these previous efforts to evaluate our current understanding of the atmospheric processes responsible for the spatial, temporal, and seasonal variability of fine inorganic PM over the Mexico City Metropolitan Area. The model domain is expanded in order to include major sources from refineries and industries, a more accurate chemical composition of the fugitive dust emissions is used, and the model predictions are evaluated against measurements from two sites; one in the urban area of Mexico City designated as T0 and located in Northeast Mexico City at the Instituto Mexicano del Petroleo (IMP), and T1, located at a suburban location approximately 32 km north of IMP (Querol et al., 2008). The evaluation focuses on the ability of PMCAMx-2008, to reproduce not only daily average concentrations but also the diurnal variation of the major inorganic aerosol components during March 2006.

2 Model description

PMCAMx-2008 uses the framework of CAMx (Environ, 2003), which models the processes of horizontal and vertical advection, horizontal and vertical dispersion, wet and dry deposition, and gas-phase chemistry. In addition, three detailed aerosol modules are used: inorganic aerosol growth (Gaydos et al., 2003; Koo et al., 2003), aqueous-phase chemistry (Fahey and Pandis, 2001), and secondary organic aerosol formation and growth (Lane et al., 2008). PMCAMx-2008 is the research version of the publicly available CAMx model.

The aerosol species treated are sulfate, nitrate, ammonium, chloride, potassium, calcium, magnesium, elemental carbon, and primary and secondary organics. The aerosol size and composition distribution is simulated using a sectional representation

Formation of semivolatile inorganic aerosols

V. A. Karydis et al.

Title Page

Abstract

Introduction

Conclusions

References

Tables

Figures



Back

Close

Full Screen / Esc

Printer-friendly Version

Interactive Discussion



across 10 size bins with the wet diameter varying from 40 nm to 40 μm . The chemical mechanism used is based on the SAPRC99 mechanism (Carter, 2000; Environ, 2003) which contains 211 reactions with 56 gases and 18 radicals.

The amount of each inorganic species transferred between the gas and aerosol phases is determined by using the hybrid approach (Capaldo et al., 2000) for aerosol thermodynamics along with ISORROPIA II (Fountoukis and Nenes, 2007) which is a computationally efficient code that treats the thermodynamics of K^+ - Ca^{2+} - Mg^{2+} - NH_4^+ - Na^+ - SO_4^{2-} - NO_3^- - Cl^- - H_2O aerosol systems. According to the hybrid method, the aerosol particles with diameters less than the threshold diameter (1 μm for the purposes of this study) are simulated assuming equilibrium while for the particles larger than the threshold diameter the improved MADM model of Pilinis et al. (2000), as extended by Gaydos et al. (2003), is used, which ensures a stable solution, regardless if the particles are completely dry, with an aqueous phase or transition between acidic and neutral conditions. Equilibrium is assumed between the gas and organic aerosol phase based on the Volatility Basis Set approach, VBS (Lane et al., 2008; Murphy and Pandis, 2009). The aerosol mass is distributed over the aerosol size distribution by using a weighting factor for each size section based on the effective surface area (condensational sink) of each size section (Pandis et al., 1993; Lurmann et al., 1997).

3 Model application

PMCAMx-2008 is used to simulate air quality in the Mexico City Metropolitan Area (MCMA) during March of 2006. The first three days of each simulation have been excluded in order to limit the effect the initial conditions have on the results. The concentrations of the aerosol components at the boundaries of the domain were chosen based on results of the GISS-II' global CTM (Racherla and Adams, 2006) for the month of March (Table 1). The modeling domain covers a 210 \times 210 km region centered in the MCMA with 3 \times 3 km grid resolution and fifteen vertical layers extending to 6 km (Fig. 1). Inputs to the model include horizontal wind components, temperature, pressure, wa-

Formation of semivolatile inorganic aerosols

V. A. Karydis et al.

Title Page

Abstract

Introduction

Conclusions

References

Tables

Figures

◀

▶

◀

▶

Back

Close

Full Screen / Esc

Printer-friendly Version

Interactive Discussion



ter vapor, vertical diffusivity, clouds, and rainfall, all computed offline by the Weather Research and Forecast (WRF) model.

The emission inventory used is based on the MCMA 2006 official emission inventory with improved dust and sodium chloride emissions, as well as new HONO emissions (0.8 % of the NO_x emissions based on Aumont et al., 2003). The improved dust emissions are the only emissions which are different for each day of simulation and they were calculated based on the algorithm of Draxler et al. (2001). The dust chemical composition including the levels of sodium, calcium, potassium, and magnesium cations, which are the reactive dust components, are determined based on the geological materials that produce fugitive dust emissions (Vega et al., 2001). Fugitive dust emitters in and around MCMA are considered to be unpaved and paved roads, agricultural soil, dried Lake, asphalt, cement plants, landfill, gravel, and tezontle soil.

4 Overview of model predictions

The predicted average ground-level concentrations of PM_{10} sulfate, nitrate, ammonium, and chloride over the period of March 2006 are shown in Fig. 2. The highest predicted sulfate concentrations are over the Tula vicinity (over $25 \mu\text{g m}^{-3}$), coming from the large SO_2 sources from the industrial complexes in the area. In the center of Mexico City, there are no major SO_2 sources, and sulfate concentrations are lower (up to $5 \mu\text{g m}^{-3}$). Nitrate is enhanced significantly in the urban area and immediate outflow (up to $3 \mu\text{g m}^{-3}$), mostly produced from local photochemistry, indicating a strong urban source. Nitrate decreases with distance from the city, due to evaporation and deposition (of HNO_3 vapor), remaining in low levels in the surroundings (lower than $1 \mu\text{g m}^{-3}$). Ammonium concentrations peak at the center of Mexico City ($2 \mu\text{g m}^{-3}$) and the Tula vicinity ($2.5 \mu\text{g m}^{-3}$) existing mainly in the form of ammonium nitrate and ammonium sulfate respectively. Predicted PM_{10} chloride concentrations are generally low (less than $0.5 \mu\text{g m}^{-3}$ in the entire model domain) with the highest values in the Texcoco dry Lake and the south area of the domain, influenced by the high south boundary conditions.

22003

Formation of semivolatile inorganic aerosols

V. A. Karydis et al.

Title Page

Abstract

Introduction

Conclusions

References

Tables

Figures

◀

▶

◀

▶

Back

Close

Full Screen / Esc

Printer-friendly Version

Interactive Discussion



The results for the coarse (PM_{1-10}) sulfate, nitrate, ammonium, chloride, sodium, calcium, potassium, and magnesium are shown in Fig. 3. The Texcoco dry Lake is a significant source of potassium ($1 \mu\text{g m}^{-3}$), magnesium ($1 \mu\text{g m}^{-3}$), sodium ($2 \mu\text{g m}^{-3}$), and calcium ($3 \mu\text{g m}^{-3}$). Coarse calcium concentrations peak around Tolteca ($7 \mu\text{g m}^{-3}$), which is located around 70 km north of the Mexico City, due to the cement industries in the area. ISORROPIA II along with the hybrid approach assist in simulating the formation of PM_{1-10} nitrate and chloride describing interactions between these anions and the cations of mineral dust. The presence of calcium coming from the Tolteca vicinity as well as the rest of the mineral cations from the Texcoco Lake resulted in the formation of a significant amount of aerosol nitrate in the coarse mode with concentrations up to $3 \mu\text{g m}^{-3}$. PM_{1-10} chloride is also high and its concentration exceeds $2 \mu\text{g m}^{-3}$ in Texcoco Lake. There is also a little ammonium in the coarse mode (less than $0.5 \mu\text{g m}^{-3}$), even if the coarse dust particles are alkaline. The soluble crustal elements increase the PM water content and thus favor the ammonium nitrate formation.

5 Model evaluation

The model predictions for PM_1 sulfate, nitrate, ammonium, and chloride were compared with measurements obtained during the MILAGRO field campaign at the T0 and T1 measurement sites (Aiken et al., 2009). The T0 monitoring station was located in the northwestern part of the basin of Mexico City. It is an urban background site influenced by road traffic fresh emissions (300 m from four major roads surrounding it), domestic and residential emissions, but also potentially influenced by local industrial emissions and from the Tula industrial area (around 60 km to the north-northwest). The model predictions for $PM_{2.5}$ sulfate, nitrate, ammonium, chloride, sodium, calcium, and magnesium were also compared with measurements that took place at T1 (Fountoukis et al., 2009). This is a suburban background site located around 50 km to the north of Mexico City, in an area isolated from major urban agglomerations but close to small populated agglomerations, and around 500 m from the closest road. The results of

Formation of semivolatile inorganic aerosols

V. A. Karydis et al.

Title Page

Abstract

Introduction

Conclusions

References

Tables

Figures

◀

▶

◀

▶

Back

Close

Full Screen / Esc

Printer-friendly Version

Interactive Discussion



the comparison between the model predictions and the measurements are depicted in Figs. 4–8.

Sulfate: The performance of the model for sulfate is encouraging in both T0 and T1 sites (Fig. 4). In T0 the average predicted PM₁ sulfate concentration is 3.7 $\mu\text{g m}^{-3}$ while the observed average was 3.5 $\mu\text{g m}^{-3}$. Both the model and the measurements show little variability in the average diurnal sulfate concentration profile. In T1 the measured PM_{2.5} sulfate concentration was variable with concentration spikes up to 15 $\mu\text{g m}^{-3}$ as the location of this station is closer to the Tula vicinity which is the major source of sulfate. The model does reproduce this behavior even if some of the spikes are not at the right times. This discrepancy between the measured and the predicted profiles is partially due to the use of the same emission inventory for SO₂ for every day. Errors in the meteorology were also identified as a major cause of some of the discrepancies between model predictions and measurements. For instance, during the 18 March the model underpredicts sulfate in both measurement sites (Fig. 4a and b). According to the measurements, the sulfate produced in Tula during the early morning of 18 March was transported to the southeast and appeared in T1 (20 $\mu\text{g m}^{-3}$) and T0 (15 $\mu\text{g m}^{-3}$) at around noon of the same day. On the other hand, there was not any peak in the predicted sulfate concentrations in T1 and T0 indicating potential problems during this period in the wind field used as input in PMCAMx-2008. The predicted average PM_{2.5} sulfate concentration in T1 is 3.3 $\mu\text{g m}^{-3}$ while the measured average is 4.4 $\mu\text{g m}^{-3}$.

Nitrate: Both PMCAMx-2008 and measurements suggest that nitrate peaks during noon at T0 (Fig. 5a) and a couple of hours later at T1 with a lower concentration (Fig. 5c). During nighttime, predicted nitrate remains low (a few $\mu\text{g m}^{-3}$) in both sites, which is consistent with the measurements. During noon, there are several high nitrate concentration (above 10 $\mu\text{g m}^{-3}$) measurement periods in the dataset during which the model tends to underpredict the nitrate levels. Comparisons of the predicted and measured diurnal nitrate profiles at T0 (Fig. 5b) suggest that the model underpredicts nitrate during noon as the predicted formation of nitrate during the early morning hours is not as rapid as the observations. This discrepancy is not the result of errors in the par-

Formation of semivolatile inorganic aerosols

V. A. Karydis et al.

Title Page

Abstract

Introduction

Conclusions

References

Tables

Figures

◀

▶

◀

▶

Back

Close

Full Screen / Esc

Printer-friendly Version

Interactive Discussion



5 titioning of the available nitric acid (Fountoukis et al., 2007) but to an underprediction of the total nitric acid. In particular, the average value of the measured total nitric acid during its peak hour (at 11:00 LT) is 4.6 ppb (Aiken et al., 2009; Zheng et al., 2008) while the average predicted total nitrate at the same hour is 3.3 ppb. This is probably
10 due to the predicted OH levels as they are slightly underestimated during early morning even though they are reasonably reproduced by the model during the rest of the day (not shown). Therefore the formation of HNO₃ during the day from the reaction of NO₂ with OH is limited in the model resulting eventually in an underprediction of the aerosol nitrate. Especially towards the last week of March 2006, the observed nitrate is
15 much higher than the predicted one, so are HONO concentrations. Li et al. (2010) and Tsimpidi et al. (2010) have shown that the HONO production is quite important for the production of OH into the early morning atmosphere in the MCMA, suggesting that a more accurate description of HONO sources is needed. The inclusion of HONO emissions, used in this application, resulted in an average increase of 0.3 μg m⁻³ in PM₁ nitrate concentration at T0 with a daily maximum of 0.9 μg m⁻³ (at 11:00 LT). Overall, the average predicted nitrate concentrations are 2.6 μg m⁻³ and 3.3 μg m⁻³ in T0 and T1 sites respectively while the observed averages were 3.5 μg m⁻³ and 3.2 μg m⁻³ respectively.

20 *Ammonium:* The ammonium predictions are quite sensitive to the ammonia emissions inventory, the predicted sulfate concentrations and the nitrate levels. The performance of the model is respectable in both sites (Fig. 6) but it underpredicts ammonium concentrations during midday in T0 (Fig. 6b), due to the underprediction in total nitric acid. In T0 the average predicted concentration is 1.7 μg m⁻³ while the observed average was 2.1 μg m⁻³. Some of the difficulty in reproducing the hourly fluctuations of
25 ammonium at T1 (Fig. 6c) is due to the sulfate predictions, as part of the ammonium in T1 exists in the aerosol phase in the form of ammonium sulfate. The predicted average PM_{2.5} ammonium concentration in T1 is 1.3 μg m⁻³ while the measured average is 1.1 μg m⁻³.

**Formation of
semivolatile
inorganic aerosols**

V. A. Karydis et al.

Title Page

Abstract

Introduction

Conclusions

References

Tables

Figures

◀

▶

◀

▶

Back

Close

Full Screen / Esc

Printer-friendly Version

Interactive Discussion



**Formation of
semivolatile
inorganic aerosols**

V. A. Karydis et al.

Title Page

Abstract

Introduction

Conclusions

References

Tables

Figures

◀

▶

◀

▶

Back

Close

Full Screen / Esc

Printer-friendly Version

Interactive Discussion



Chloride: Both observations and predictions suggest that chloride concentrations remain at low levels (up to $0.5 \mu\text{g m}^{-3}$) most of the time in both the T0 and T1 sites (Fig. 7). Nevertheless, there are some measured major spikes at T0 site during the morning rush hours that the model is unable to reproduce (Fig. 7a). These spikes were observed mostly in the last week of the campaign. Given that the model uses the same HCl emissions for every week day, it should be investigated if these emissions were, for some reason, higher during this week. During this period there is a clear decrease in the number of fires due to higher precipitation and humidity (Fast et al., 2007). Surprisingly enough, measured chloride is higher during this low fire period, which indicates that despite the emission of chloride by fires (DeCarlo et al., 2008), urban sources and/or favorable partitioning conditions may be more important for this species in the MCMA. Comparisons of the predicted and measured diurnal profiles at T0 (Fig. 7b) suggest that the model underpredicts chloride. The average predicted concentration is $0.25 \mu\text{g m}^{-3}$ while the observed average was $0.35 \mu\text{g m}^{-3}$. Given that the AMS measures only non refractory chloride, the model underprediction of the ambient chloride concentration is probably greater. Aiken et al. (2009) suggest that approximately two thirds of the chloride is due to NH_4Cl or species of similarly high volatility, while the rest may be due to more refractory species such as PbCl_2 that are not simulated by the model. In T1, the predicted average $\text{PM}_{2.5}$ chloride concentration is $0.3 \mu\text{g m}^{-3}$ while the measured average is $0.4 \mu\text{g m}^{-3}$.

Dust components: Measurements of $\text{PM}_{2.5}$ sodium, calcium, and magnesium were only available at T1. PMCAMx-2008 shows on average a reasonable performance for these three dust components (Fig. 8). However, there is a tendency towards over-prediction, especially for calcium (Fig. 8b), indicating a possible overestimation of the dust emissions that PMCAMx-2008 uses and probably errors in the contributions of the individual dust components or their size distribution. The predicted peaks at T1 for sodium, calcium, and magnesium are in the $1 \mu\text{g m}^{-3}$, $10 \mu\text{g m}^{-3}$, and $0.5 \mu\text{g m}^{-3}$ respectively, while the measured peaks are in the range of $0.5 \mu\text{g m}^{-3}$ for sodium, $3 \mu\text{g m}^{-3}$ for calcium, and $0.3 \mu\text{g m}^{-3}$ for magnesium. Despite the above weakness,

the model captures relative well not only the daily average concentrations of the dust components, but also their average diurnal variation, as both the predicted and the measured profiles are flat with almost constant concentration. The daily average predicted concentrations of PM_{2.5} sodium, calcium, and magnesium at T1 are 0.4 μg m⁻³, 1 μg m⁻³, and 0.15 μg m⁻³ respectively, while the average measured concentrations of the same species are 0.3 μg m⁻³, 0.7 μg m⁻³ and 0.15 μg m⁻³ respectively.

6 Sensitivity to inorganic aerosol dynamics

To estimate the effects of the hybrid aerosol thermodynamic approach on the formation of the semi-volatile inorganic aerosol components, the predictions of the model using the hybrid approach were compared against those using the equilibrium approach for the simulation of the partitioning of semivolatile inorganic PM components. The concentration difference in the fine and coarse mode between the predictions of these two modeling approaches for nitrate is shown in Fig. 9. Positive concentrations reflect increases due to the use of the hybrid approach.

Assuming bulk equilibrium between the gas and the aerosol phase results in an increase of the predicted PM₁ nitrate up to 2.5 μg m⁻³ while, at the same time, the nitrate concentration on the coarse mode decreases by an equal amount. This significant change on the results is due to the fact that the bulk equilibrium algorithm distributes most of the total PM nitrate to the fine mode (approximately 90%) that has most of the surface area. In the hybrid approach, the coarse fraction continues to absorb nitric acid vapors, even after the small particles achieve equilibrium, thus lowering the nitric acid gas-phase concentration. The smallest sections then lose mass as evaporation is required to maintain equilibrium with the gas phase. As a result the predicted coarse nitrate using the hybrid approach represents 55% on average of the total PM nitrate. Therefore, the hybrid approach is considered essential in order to accurately simulate the size distribution of the inorganic aerosols.

Formation of semivolatile inorganic aerosols

V. A. Karydis et al.

Title Page

Abstract

Introduction

Conclusions

References

Tables

Figures

◀

▶

◀

▶

Back

Close

Full Screen / Esc

Printer-friendly Version

Interactive Discussion



7 Sensitivity to emissions of inorganic aerosol precursors

In order to estimate the response of fine PM components to changes in anthropogenic emissions in Mexico City, three control strategies are examined separately, a 50 % reduction of SO₂, a 50 % reduction of NH₃, and a 50 % reduction of NO_x emissions.

5 These should be viewed as sensitivity tests as they do not correspond to actual emission control strategies. The results of these simulations are compared to the results of the base case simulation to examine the effectiveness of these strategies in the reduction of PM₁ sulfate, nitrate, and ammonium concentrations.

The predicted changes in ground-level concentrations of the inorganic aerosols after a 50 % reduction of SO₂ emissions are shown in Fig. 10. Sulfate decreases by approximately 0.5 μg m⁻³ (less than 5 %) in the Tula vicinity, where it has the highest concentration, while in the center of Mexico City the reduction of sulfate is approximately 0.3 μg m⁻³ (~10 %). The highest reduction on the hourly average concentration is 8 μg m⁻³ (25 %) in Tula. This extremely non linear response of sulfate concentration to the reduction of SO₂ emissions is in contrast with the findings of Tsimpidi et al. (2007) where sulfate concentration on the Eastern US varied linearly with SO₂ emissions, especially during the summer season. The main difference between the atmosphere of Mexico City and the eastern US is the concentration of SO₂ which in MCMA is predicted to be more than 10 times higher than in the eastern US. Therefore, the oxidant concentration in the area is not sufficient for the SO₂ oxidation to SO₄²⁻ and the production of the latter is more controlled by the availability of oxidants than of SO₂. Nitrate concentration increases up to 0.1 μg m⁻³ (10 %) after the reduction of SO₂ emissions while the maximum increase on the hourly average concentration is 0.6 μg m⁻³ (25 %). This increase is attributed to the increase of free ammonia, after the reduction of sulfate, which reacted with HNO₃ to form additional particulate nitrate. Ammonium concentration decreases by 0.1 μg m⁻³ (5–10 %) in the center of Mexico City and the hourly maximum concentration decreases by 1 μg m⁻³ (40 %). The reduction of ammonium in Tula is very small (0.02 μg m⁻³ or 0.01 %) as ammonium sulfate

Formation of semivolatile inorganic aerosols

V. A. Karydis et al.

Title Page

Abstract

Introduction

Conclusions

References

Tables

Figures

◀

▶

◀

▶

Back

Close

Full Screen / Esc

Printer-friendly Version

Interactive Discussion



represents a small fraction ($\sim 20\%$) of total sulfate mass in the area.

The predicted changes in ground-level concentrations of the inorganic aerosols after a 50% reduction of NH_3 emissions are shown in Fig. 11. Sulfate concentration is not sensitive to changes of ammonia emissions as even in environments with low NH_3 , sulfate still exists in the aerosol phase in the form of ammonium bisulfate or as H_2SO_4 . In the center of Mexico City, after the 50% reduction of NH_3 emissions, nitrate and ammonium decreases by $1 \mu\text{g m}^{-3}$ (35%) and $0.3 \mu\text{g m}^{-3}$ (20%) respectively. The highest reduction of ammonium concentration is predicted in Tula and is up to $1 \mu\text{g m}^{-3}$ (35%). The highest hourly average concentration of nitrate, located in Mexico City center, and ammonium, located in Tula, is reduced by $10 \mu\text{g m}^{-3}$ (60%) and $4 \mu\text{g m}^{-3}$ (45%) respectively.

The predicted changes in ground-level concentrations of the inorganic aerosols after a 50% reduction of NO_x emissions are shown in Fig. 12. In the center of Mexico City, the decrease of NO_x emissions results in lower OH radical and ozone concentrations and consequently a decrease of sulfate concentration levels. In particular, sulfate decreases by up to $0.2 \mu\text{g m}^{-3}$ (7%) with an hourly maximum of $3.5 \mu\text{g m}^{-3}$ (35%). In Tula, a reduction of NO_x concentrations results in an increase of OH and O_3 concentrations and, as a result, sulfate concentration increases by $0.3 \mu\text{g m}^{-3}$ (2%) with an hourly maximum of $7 \mu\text{g m}^{-3}$ (15%). Nitrate decreases by $1 \mu\text{g m}^{-3}$ (35%), with an hourly maximum of $7.5 \mu\text{g m}^{-3}$ (50%), as NO_x is the main precursor of HNO_3 in the atmosphere. Finally, the simultaneously decrease of both nitrate and sulfate concentration levels in Mexico City resulted in a $0.3 \mu\text{g m}^{-3}$ (20%) decrease of ammonium concentration, with an hourly maximum of $2 \mu\text{g m}^{-3}$ (45%).

8 Conclusions

A detailed three-dimensional chemical transport model (PMCAMx-2008), which contains an advance thermodynamic description of the semivolatile inorganic components, is presented and applied during the MILAGRO-2006 campaign in the Mexico

22010

Formation of semivolatile inorganic aerosols

V. A. Karydis et al.

Title Page

Abstract

Introduction

Conclusions

References

Tables

Figures

◀

▶

◀

▶

Back

Close

Full Screen / Esc

Printer-friendly Version

Interactive Discussion



City Metropolitan Area. The model predictions were compared against measurements taken from the T0 site, located in the urban area of Mexico City, and from T1 site, located at a suburban area. Overall, PMCAMx-2008 was able to reproduce both the daily average concentrations and the diurnal variation of the major inorganic aerosol components. A number of conclusions arise from our analysis:

- Sulfate is regional in nature with clear influences from the large SO₂ sources in the industrial complex in Tula, while the urban area is not a major source of sulfate.
- Nitrate is enhanced significantly in the urban area and immediate outflow (up to 3 μg m⁻³), mostly produced from local photochemistry, indicating a strong urban source. It decreases with distance from the city, due to evaporation and deposition, remaining in low levels in the surroundings (lower than 1 μg m⁻³).
- There is significant need for improvement of the simulation of HONO formation in the early morning.
- Ammonium concentrations peak at the center of Mexico City and the Tula vicinity (3 μg m⁻³) existing mainly in the form of ammonium nitrate and ammonium sulfate respectively.
- The Texcoco dry Lake is a significant source of potassium (up to 1 μg m⁻³), magnesium (1 μg m⁻³), sodium (2 μg m⁻³), and calcium (3 μg m⁻³) that influences the PM concentrations in the areas to the east and northeast of the city.
- Calcium concentrations peak near Toluca (up to 7 μg m⁻³) as a result of emissions from the cement industries in the area.
- ISORROPIA-II along with the hybrid approach assist the model in simulating the formation of the semivolatile inorganic PM as it includes interactions with the mineral dust components.

Formation of semivolatile inorganic aerosols

V. A. Karydis et al.

Title Page

Abstract

Introduction

Conclusions

References

Tables

Figures

◀

▶

◀

▶

Back

Close

Full Screen / Esc

Printer-friendly Version

Interactive Discussion



Formation of semivolatile inorganic aerosols

V. A. Karydis et al.

Title Page

Abstract

Introduction

Conclusions

References

Tables

Figures

◀

▶

◀

▶

Back

Close

Full Screen / Esc

Printer-friendly Version

Interactive Discussion



- The use of the same emission inventory for every week day introduces errors in predicting the variations of the concentration of the major inorganic components.
- The model underestimates the OH concentrations and thus the formation of HNO₃. The lack of HNO₃ results in an underestimation of the ammonium nitrate during the day.
- The predicted unrealistic high peaks of dust components concentrations at T1 site indicate a possible overestimation of the dust emissions.
- A 50 % reduction of SO₂ emissions leads to a decrease of average PM₁ sulfate and ammonium concentrations up to 0.5 μg m⁻³ and 0.1 μg m⁻³ respectively, and to an increase of PM₁ nitrate concentration up to 0.1 μg m⁻³.
- A 50 % reduction of NH₃ emissions leads to a decrease of PM₁ nitrate and ammonium concentrations up to 1 μg m⁻³ in Mexico City center and 1 μg m⁻³ in Tula respectively. The ammonium concentration reduction in the center of Mexico City is up to 0.3 μg m⁻³. Sulfate concentration is not sensitive to changes of ammonia emissions.
- A 50 % reduction of NO_x emissions leads to a decrease of PM₁ nitrate and ammonium concentrations up to 1 μg m⁻³ and 0.3 μg m⁻³ respectively. PM₁ sulfate concentration decreases by 0.2 μg m⁻³ in Mexico City and increases by 0.3 μg m⁻³ in Tula.

Acknowledgements. This research was supported by the European Union and the 7th framework programme under the project MEGAPOLI (Grant agreement no./ 212520). LTM would like to acknowledge support from NSF (ATM-0528227).

References

- Aiken, A. C., Salcedo, D., Cubison, M. J., Huffman, J. A., DeCarlo, P. F., Ulbrich, I. M., Docherty, K. S., Sueper, D., Kimmel, J. R., Worsnop, D. R., Trimborn, A., Northway, M., Stone, E. A., Schauer, J. J., Volkamer, R. M., Fortner, E., de Foy, B., Wang, J., Laskin, A., Shutthanandan, V., Zheng, J., Zhang, R., Gaffney, J., Marley, N. A., Paredes-Miranda, G., Arnott, W. P., Molina, L. T., Sosa, G., and Jimenez, J. L.: Mexico City aerosol analysis during MILAGRO using high resolution aerosol mass spectrometry at the urban supersite (T0) – Part 1: Fine particle composition and organic source apportionment, *Atmos. Chem. Phys.*, 9, 6633–6653, doi:10.5194/acp-9-6633-2009, 2009.
- 5
- 10 Ansari, A. S. and Pandis, S. N.: Response of inorganic PM to precursor concentrations, *Environ. Sci. Technol.*, 32, 2706–2714, 1998.
- Ansari, A. S. and Pandis, S. N.: Prediction of multicomponent inorganic atmospheric aerosol behavior, *Atmos. Environ.*, 33, 745–757, 1999a.
- Ansari, A. S. and Pandis, S. N.: An analysis of four models predicting the partitioning of semivolatile inorganic aerosol components, *Aerosol Sci. Technol.*, 31, 129–153, 1999b.
- 15
- Ansari, A. S. and Pandis, S. N.: The effect of metastable equilibrium states on the partitioning of nitrate between the gas and aerosol phases, *Atmos. Environ.*, 34, 157–168, 2000.
- Aumont, B., Chervier, F., and Laval, S.: Contribution of HONO sources to the $\text{NO}_x/\text{HO}_x/\text{O}^{-3}$ chemistry in the polluted boundary layer, *Atmos. Environ.*, 37, 487–498, 2003.
- 20
- Bassett, M. and Seinfeld, J. H.: Atmospheric equilibrium-model of sulfate and nitrate aerosols, *Atmos. Environ.*, 17, 2237–2252, 1983.
- Capaldo, K. P., Pilinis, C., and Pandis, S. N.: A computationally efficient hybrid approach for dynamic gas/aerosol transfer in air quality models, *Atmos. Environ.*, 34, 3617–3627, 2000.
- Carter, W. P. L.: Implementation of the SAPRC-99 chemical mechanism into the models-3 framework: <http://citeseerx.ist.psu.edu/viewdoc/download?doi=10.1.1.25.293&rep=rep1&type=pdf>, last access: 25 February 2008, 2000.
- 25
- 30
- Chow, J. C. and Egami, R. T.: San Joaquin Valley 1995 integrated monitoring study: Documentation, evaluation, and descriptive data analysis of PM₁₀, PM_{2.5}, and precursor gas measurements. Technical Support Studies No. 4 and No. 8. Final Report prepared for the Technical Support Division, California Air Resources Board, Sacramento, CA by Desert Research Institute, Reno, NV, DRI Document No. 5460.1F1, 1997.

Formation of semivolatile inorganic aerosols

V. A. Karydis et al.

Title Page

Abstract

Introduction

Conclusions

References

Tables

Figures

◀

▶

◀

▶

Back

Close

Full Screen / Esc

Printer-friendly Version

Interactive Discussion



**Formation of
semivolatile
inorganic aerosols**

V. A. Karydis et al.

Title Page

Abstract

Introduction

Conclusions

References

Tables

Figures

◀

▶

◀

▶

Back

Close

Full Screen / Esc

Printer-friendly Version

Interactive Discussion



Clegg, S. L., Brimblecombe, P., and Wexler, A. S.: Thermodynamic model of the system $\text{H}^+ - \text{NH}_4^+ - \text{SO}_4^{2-} - \text{NO}_3^- - \text{H}_2\text{O}$ at tropospheric temperatures, *J. Phys. Chem. A*, 102, 2137–2154, 1998a.

5 Clegg, S. L., Brimblecombe, P., and Wexler, A. S.: Thermodynamic model of the system $\text{H}^+ - \text{NH}_4^+ - \text{Na}^+ - \text{SO}_4^{2-} - \text{NB}_3^- - \text{Cl}^- - \text{H}_2\text{O}$ at 298.15 K, *J. Phys. Chem. A*, 102, 2155–2171, 1998b.

DeCarlo, P. F., Dunlea, E. J., Kimmel, J. R., Aiken, A. C., Sueper, D., Crouse, J., Wennberg, P. O., Emmons, L., Shinzuka, Y., Clarke, A., Zhou, J., Tomlinson, J., Collins, D. R., Knapp, D., Weinheimer, A. J., Montzka, D. D., Campos, T., and Jimenez, J. L.: Fast airborne aerosol size and chemistry measurements above Mexico City and Central Mexico during the MILAGRO

10 campaign, *Atmos. Chem. Phys.*, 8, 4027–4048, doi:10.5194/acp-8-4027-2008, 2008.

Draxler, R. R., Gillette, D. A., Kirkpatrick, J. S., and Heller, J.: Estimating PM_{10} air concentrations from dust storms in Iraq, Kuwait and Saudi Arabia, *Atmos. Environ.*, 35, 4315–4330, 2001.

15 Environ: User's guide to the comprehensive air quality model with extensions (CAMx). Version 4.02. Report prepared by ENVIRON International Corporation, Novato, CA, USA, 2003.

Fahey, K. M. and Pandis, S. N.: Optimizing model performance: variable size resolution in cloud chemistry modeling, *Atmos. Environ.*, 35, 4471–4478, 2001.

Fast, J. D., de Foy, B., Rosas, F. A., Caetano, E., Carmichael, G., Emmons, L., McKenna, D., Mena, M., Skamarock, W., Tie, X., Coulter, R. L., Barnard, J. C., Wiedinmyer, C., and Madronich, S.: A meteorological overview of the MILAGRO field campaigns, *Atmos. Chem. Phys.*, 7, 2233–2257, doi:10.5194/acp-7-2233-2007, 2007.

20 Fountoukis, C. and Nenes, A.: ISORROPIA II: a computationally efficient thermodynamic equilibrium model for $\text{K}^+ - \text{Ca}^{2+} - \text{Mg}^{2+} - \text{NH}_4^+ - \text{Na}^+ - \text{SO}_4^{2-} - \text{NO}_3^- - \text{Cl}^- - \text{H}_2\text{O}$ aerosols, *Atmos. Chem. Phys.*, 7, 4639–4659, doi:10.5194/acp-7-4639-2007, 2007.

Fountoukis, C., Nenes, A., Sullivan, A., Weber, R., Van Reken, T., Fischer, M., Matias, E., Moya, M., Farmer, D., and Cohen, R. C.: Thermodynamic characterization of Mexico City aerosol during MILAGRO 2006, *Atmos. Chem. Phys.*, 9, 2141–2156, doi:10.5194/acp-9-2141-2009, 2009.

30 Gaydos, T. M., Koo, B., Pandis, S. N., and Chock, D. P.: Development and application of an efficient moving sectional approach for the solution of the atmospheric aerosol condensation/evaporation equations, *Atmos. Environ.*, 37, 3303–3316, 10.1016/s1352-2310(03)00267-x, 2003.

**Formation of
semivolatile
inorganic aerosols**

V. A. Karydis et al.

Title Page

Abstract

Introduction

Conclusions

References

Tables

Figures

◀

▶

◀

▶

Back

Close

Full Screen / Esc

Printer-friendly Version

Interactive Discussion



Hildemann, L. M., Russell, A. G., and Cass, G. R.: Ammonia and nitric-acid concentrations in equilibrium with atmospheric aerosols – experiment vs theory, *Atmos. Environ.*, **18**, 1737–1750, 1984.

Hodzic, A., Jimenez, J. L., Madronich, S., Aiken, A. C., Bessagnet, B., Curci, G., Fast, J., Lamarque, J. F., Onasch, T. B., Roux, G., Schauer, J. J., Stone, E. A., and Ulbrich, I. M.: Modeling organic aerosols during MILAGRO: importance of biogenic secondary organic aerosols, *Atmos. Chem. Phys.*, **9**, 6949–6981, doi:10.5194/acp-9-6949-2009, 2009.

Hodzic, A., Jimenez, J. L., Madronich, S., Canagaratna, M. R., DeCarlo, P. F., Kleinman, L., and Fast, J.: Modeling organic aerosols in a megacity: potential contribution of semi-volatile and intermediate volatility primary organic compounds to secondary organic aerosol formation, *Atmos. Chem. Phys.*, **10**, 5491–5514, doi:10.5194/acp-10-5491-2010, 2010.

Jacobson, M. Z., Tabazadeh, A., and Turco, R. P.: Simulating equilibrium within aerosols and nonequilibrium between gases and aerosols, *J. Geophys. Res.-Atmos.*, **101**, 9079–9091, 1996.

Jacobson, M. Z.: Development and application of a new air pollution modeling system .2. Aerosol module structure and design, *Atmos. Environ.*, **31**, 131–144, 1997a.

Jacobson, M. Z.: Numerical techniques to solve condensational and dissolutional growth equations when growth is coupled to reversible reactions, *Aerosol Sci. Technol.*, **27**, 491–498, 1997b.

Jacobson, M. Z.: Studying the effects of calcium and magnesium on size-distributed nitrate and ammonium with EQUISOLV II, *Atmos. Environ.*, **33**, 3635–3649, 1999.

Karydis, V. A., Tsimpidi, A. P., Fountoukis, C., Nenes, A., Zavala, M., Lei, W. F., Molina, L. T., and Pandis, S. N.: Simulating the fine and coarse inorganic particulate matter concentrations in a polluted megacity, *Atmos. Environ.*, **44**, 608–620, doi:10.1016/j.atmosenv.2009.11.023, 2010.

Kim, Y. P. and Seinfeld, J. H.: Atmospheric gas-aerosol equilibrium .3. Thermodynamics of crustal elements Ca^{2+} , K^+ , and Mg^{2+} , *Aerosol Sci. Technol.*, **22**, 93–110, 1995.

Kim, Y. P., Seinfeld, J. H., and Saxena, P.: Atmospheric gas aerosol equilibrium .1. Thermodynamic model, *Aerosol Sci. Technol.*, **19**, 157–181, 1993a.

Kim, Y. P., Seinfeld, J. H., and Saxena, P.: Atmospheric gas-aerosol equilibrium .2. Analysis of common approximations and activity-coefficient calculation methods, *Aerosol Sci. Technol.*, **19**, 182–198, 1993b.

**Formation of
semivolatile
inorganic aerosols**

V. A. Karydis et al.

Title Page

Abstract

Introduction

Conclusions

References

Tables

Figures



Back

Close

Full Screen / Esc

Printer-friendly Version

Interactive Discussion



Koo, B. Y., Ansari, A. S., and Pandis, S. N.: Integrated approaches to modeling the organic and inorganic atmospheric aerosol components, *Atmos. Environ.*, 37, 4757–4768, doi:10.1016/j.atmosenv.2003.08.016, 2003.

5 Kumar, N., Lurmann, F. W., Pandis, S. N., and Ansari, A. S.: Final Report: analysis of atmospheric chemistry during 1995 integrated monitoring study. Final Report Prepared for the California Air Resources Board, Sacramento, CA by Sonoma Technology Inc., Santa Rosa, CA, USA, STI-997214-1791-DFR, 1998.

Lane, T. E., Donahue, N. M., and Pandis, S. N.: Simulating secondary organic aerosol formation using the volatility basis-set approach in a chemical transport model, *Atmos. Environ.*, 42, 7439–7451, doi:10.1016/j.atmosenv.2008.06.026, 2008.

10 Lawson, D. R.: The southern california air-quality study, *J. Air Waste Manage. Assoc.*, 40, 156–165, 1990.

Li, G., Lei, W., Zavala, M., Volkamer, R., Dusanter, S., Stevens, P., and Molina, L. T.: Impacts of HONO sources on the photochemistry in Mexico City during the MCMA-2006/MILAGO Campaign, *Atmos. Chem. Phys.*, 10, 6551–6567, doi:10.5194/acp-10-6551-2010, 2010.

15 Li, G., Zavala, M., Lei, W., Tsimpidi, A. P., Karydis, V. A., Pandis, S. N., Canagaratna, M. R., and Molina, L. T.: Simulations of organic aerosol concentrations in Mexico City using the WRF-CHEM model during the MCMA-2006/MILAGRO campaign, *Atmos. Chem. Phys.*, 11, 3789–3809, doi:10.5194/acp-11-3789-2011, 2011.

20 Lurmann, F. W., Wexler, A. S., Pandis, S. N., Musarra, S., Kumar, N., and Seinfeld, J. H.: Modelling urban and regional aerosols .2. Application to California's South Coast Air Basin, *Atmos. Environ.*, 31, 2695–2715, 1997.

Meng, Z. Y., Seinfeld, J. H., Saxena, P., and Kim, Y. P.: Atmospheric gas-aerosol equilibrium .4. Thermodynamics of carbonates, *Aerosol Sci. Technol.*, 23, 131–154, 1995.

25 Meng, Z. Y., Dabdub, D., and Seinfeld, J. H.: Size-resolved and chemically resolved model of atmospheric aerosol dynamics, *J. Geophys. Res.-Atmos.*, 103, 3419–3435, 1998.

Molina, L. T. and Molina, M. J.: *Air Quality in the Mexico Megacity: An Integrated Assessment*, Kluwer Academic Publishers, The Netherlands, 2002.

30 Molina, L. T., Madronich, S., Gaffney, J. S., Apel, E., de Foy, B., Fast, J., Ferrare, R., Herndon, S., Jimenez, J. L., Lamb, B., Osornio-Vargas, A. R., Russell, P., Schauer, J. J., Stevens, P. S., Volkamer, R., and Zavala, M.: An overview of the MILAGRO 2006 Campaign: Mexico City emissions and their transport and transformation, *Atmos. Chem. Phys.*, 10, 8697–8760, doi:10.5194/acp-10-8697-2010, 2010.

- Murphy, B. N. and Pandis, S. N.: Simulating the Formation of Semivolatile Primary and Secondary Organic Aerosol in a Regional Chemical Transport Model, *Environ. Sci. Technol.*, 43, 4722–4728, doi:10.1021/es803168a, 2009.
- Nenes, A., Pandis, S. N., and Pilinis, C.: ISORROPIA: A new thermodynamic equilibrium model for multiphase multicomponent inorganic aerosols, *Aqua. Geochem.*, 4, 123–152, 1998.
- Nenes, A., Pandis, S. N., and Pilinis, C.: Continued development and testing of a new thermodynamic aerosol module for urban and regional air quality models, *Atmos. Environ.*, 33, 1553–1560, 1999.
- Pandis, S. N., Wexler, A. S., and Seinfeld, J. H.: Secondary organic aerosol formation and transport .2. Predicting the ambient secondary organic aerosol-size distribution, *Atmos. Environ.*, 27, 2403–2416, 1993.
- Pilinis, C. and Seinfeld, J. H.: Continued development of a general equilibrium-model for inorganic multicomponent atmospheric aerosols, *Atmos. Environ.*, 21, 2453–2466, 1987.
- Pilinis, C. and Seinfeld, J. H.: Development and evaluation of an eulerian photochemical gas aerosol model, *Atmos. Environ.*, 22, 1985–2001, 1988.
- Pilinis, C., Capaldo, K. P., Nenes, A., and Pandis, S. N.: MADM – A new multicomponent aerosol dynamics model, *Aerosol Sci. Technol.*, 32, 482–502, 2000.
- Racherla, P. N. and Adams, P. J.: Sensitivity of global tropospheric ozone and fine particulate matter concentrations to climate change, *J. Geophys. Res.-Atmos.*, 111, D24103, doi:10.1029/2005jd006939, 2006.
- Russell, A. G., McCue, K. F., and Cass, G. R.: Mathematical-modeling of the formation of nitrogen-containing air-pollutants .1. Evaluation of an eulerian photochemical model, *Environ. Sci. Technol.*, 22, 263–270, 1988.
- Saxena, P., Hudischewskyj, A. B., Seigneur, C., and Seinfeld, J. H.: A comparative-study of equilibrium approaches to the chemical characterization of secondary aerosols, *Atmos. Environ.*, 20, 1471–1483, 1986.
- Seinfeld, J. H., and Pandis, S. N.: *Atmospheric Chemistry and Physics: From Air Pollution to Climate Change*, Second ed., John Wiley & Sons, Inc., Hoboken, New Jersey, USA, 2006.
- Tanner, R. L.: An ambient experimental-study of phase-equilibrium in the atmospheric system–aerosol H^+ , NH_4^+ , SO_4^{2-} , NO_3^- - $\text{NH}_3(\text{g})$, $\text{HNO}_3(\text{g})$, *Atmos. Environ.*, 16, 2935–2942, 1982.
- Tie, X., Madronich, S., Li, G., Ying, Z., Weinheimer, A., Apel, E., and Campos, T.: Simulation of Mexico City plumes during the MIRAGE-Mex field campaign using the WRF-Chem model, *Atmos. Chem. Phys.*, 9, 4621–4638, doi:10.5194/acp-9-4621-2009, 2009.

**Formation of
semivolatile
inorganic aerosols**

V. A. Karydis et al.

Title Page

Abstract

Introduction

Conclusions

References

Tables

Figures

◀

▶

◀

▶

Back

Close

Full Screen / Esc

Printer-friendly Version

Interactive Discussion



**Formation of
semivolatile
inorganic aerosols**

V. A. Karydis et al.

[Title Page](#)[Abstract](#)[Introduction](#)[Conclusions](#)[References](#)[Tables](#)[Figures](#)[⏪](#)[⏩](#)[◀](#)[▶](#)[Back](#)[Close](#)[Full Screen / Esc](#)[Printer-friendly Version](#)[Interactive Discussion](#)

- Tsimpidi, A. P., Karydis, V. A., and Pandis, S. N.: Response of inorganic fine particulate matter to emission changes of sulfur dioxide and ammonia: The eastern United States as a case study, *J. Air Waste Manage. Assoc.*, 57, 1489–1498, doi:10.3155/1047-3289.57.12.1489, 2007.
- 5 Tsimpidi, A. P., Karydis, V. A., Zavala, M., Lei, W., Molina, L., Ulbrich, I. M., Jimenez, J. L., and Pandis, S. N.: Evaluation of the volatility basis-set approach for the simulation of organic aerosol formation in the Mexico City metropolitan area, *Atmos. Chem. Phys.*, 10, 525–546, doi:10.5194/acp-10-525-2010, 2010.
- Tsimpidi, A. P., Karydis, V. A., Zavala, M., Lei, W., Bei, N., Molina, L., and Pandis, S. N.:
10 Sources and production of organic aerosol in Mexico City: insights from the combination of a chemical transport model (PMCAMx-2008) and measurements during MILAGRO, *Atmos. Chem. Phys.*, 11, 5153–5168, doi:10.5194/acp-11-5153-2011, 2011.
- Vega, E., Mugica, V., Reyes, E., Sanchez, G., Chow, J. C., and Watson, J. G.: Chemical composition of fugitive dust emitters in Mexico City, *Atmos. Environ.*, 35, 4033–4039, 2001.
- 15 Watson, J. G., Chow, J. C., Lurmann, F. W., and Musarra, S. P.: Ammonium-nitrate, nitric-acid, and ammonia equilibrium in wintertime Phoenix, Arizona, *J. Air Waste Manage. Assoc.*, 44, 405-412, 1994.
- Wexler, A. S. and Seinfeld, J. H.: 2nd-generation inorganic aerosol model, *Atmos. Environ.*, 25, 2731–2748, 1991.
- 20 Ying, Z., Tie, X., Madronich, S., Li, G., and Massie, S.: Simulation of regional dust and its effect on photochemistry in the Mexico City area during MILAGRO experiment, *Atmos. Environ.*, 45, 2549–2558, 2011.
- Zhang, J., Chameides, W. L., Weber, R., Cass, G., Orsini, D., Edgerton, E., Jongejan, P., and Slanina, J.: An evaluation of the thermodynamic equilibrium assumption for fine particulate composition: Nitrate and ammonium during the 1999 Atlanta Supersite Experiment, *J. Geophys. Res.-Atmos.*, 108, 8414, doi:10.1029/2001jd001592, 2002.
- 25 Zhang, Y., Seigneur, C., Seinfeld, J. H., Jacobson, M., Clegg, S. L., and Binkowski, F. S.: A comparative review of inorganic aerosol thermodynamic equilibrium modules: similarities, differences, and their likely causes, *Atmos. Environ.*, 34, 117–137, 2000.
- 30 Zhang, Y., Dubey, M. K., Olsen, S. C., Zheng, J., and Zhang, R.: Comparisons of WRF/Chem simulations in Mexico City with ground-based RAMA measurements during the 2006-MILAGRO, *Atmos. Chem. Phys.*, 9, 3777–3798, doi:10.5194/acp-9-3777-2009, 2009.

Zheng, J., Zhang, R., Fortner, E. C., Volkamer, R. M., Molina, L., Aiken, A. C., Jimenez, J. L., Gaeggeler, K., Dommen, J., Dusanter, S., Stevens, P. S., and Tie, X.: Measurements of HNO₃ and N₂O₅ using ion drift-chemical ionization mass spectrometry during the MILAGRO/MCMA-2006 campaign, *Atmos. Chem. Phys.*, 8, 6823–6838, doi:10.5194/acp-8-6823-2008, 2008.

5

22019

ACPD

11, 21995–22032, 2011

Formation of semivolatile inorganic aerosols

V. A. Karydis et al.

Title Page

Abstract

Introduction

Conclusions

References

Tables

Figures

⏪

⏩

◀

▶

Back

Close

Full Screen / Esc

Printer-friendly Version

Interactive Discussion



Formation of semivolatile inorganic aerosols

V. A. Karydis et al.

Title Page

Abstract

Introduction

Conclusions

References

Tables

Figures

◀

▶

◀

▶

Back

Close

Full Screen / Esc

Printer-friendly Version

Interactive Discussion



Table 1. Aerosol concentrations ($\mu\text{g m}^{-3}$) at the boundaries of the domain.

Species	South Boundary	West Boundary	East Boundary	North Boundary
Sulfate	1.7	3.0	2.6	1.4
Ammonium	0.3	1.0	1.0	0.4
Nitrate	1.4	0.7	1.2	1.2
Chloride	3.2	0.8	1.1	1.1
Sodium	2.7	0.7	1	0.9
Calcium	0.1	0.1	0.1	0.1
Magnesium	0.2	0.1	0.1	0.1
Potassium	0.1	0.1	0.1	0.1
Organic Mass	7.0	8.0	11.5	5.0

**Formation of
semivolatile
inorganic aerosols**

V. A. Karydis et al.

Title Page

Abstract

Introduction

Conclusions

References

Tables

Figures

◀

▶

◀

▶

Back

Close

Full Screen / Esc

Printer-friendly Version

Interactive Discussion



Fig. 1. The modeling domain for the Mexico City Metropolitan Area during the MILAGRO campaign. It also shows the locations of the monitoring stations during the campaign.

**Formation of
semivolatile
inorganic aerosols**

V. A. Karydis et al.

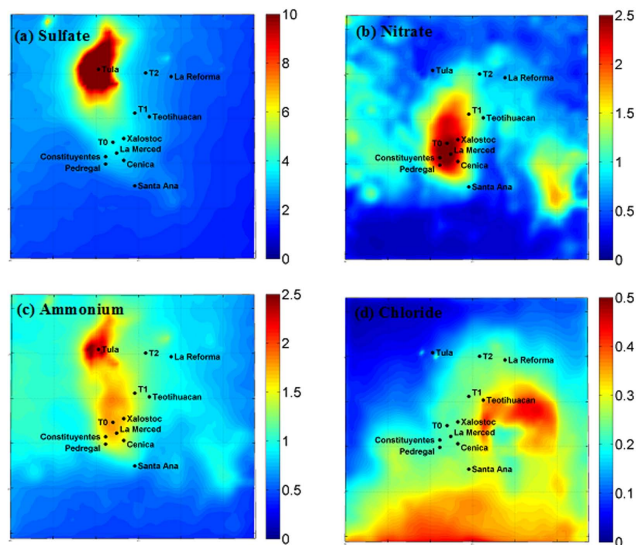


Fig. 2. Predicted average ground level concentrations of PM₁ (a) sulfate, (b) nitrate, (c) ammonium, and (d) chloride during 4–30 March 2006.

Title Page

Abstract

Introduction

Conclusions

References

Tables

Figures

◀

▶

◀

▶

Back

Close

Full Screen / Esc

Printer-friendly Version

Interactive Discussion



Formation of semivolatile inorganic aerosols

V. A. Karydis et al.

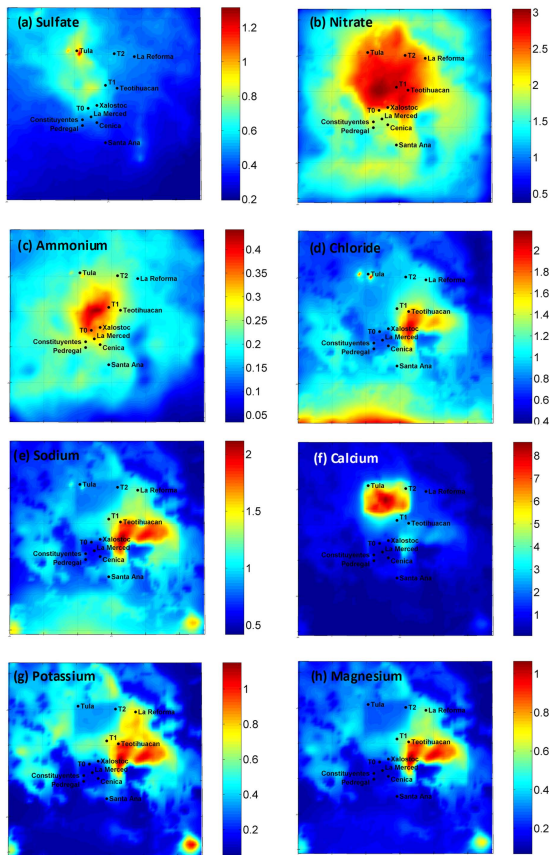


Fig. 3. Predicted average ground level concentrations of PM_{1–10} **(a)** sulfate, **(b)** nitrate, **(c)** ammonium, **(d)** chloride, **(e)** sodium, **(f)** calcium, **(g)** potassium, and **(h)** magnesium ($\mu\text{g m}^{-3}$) during 4–30 March 2006.

Title Page

Abstract Introduction

Conclusions References

Tables Figures

◀ ▶

◀ ▶

Back Close

Full Screen / Esc

Printer-friendly Version

Interactive Discussion



**Formation of
semivolatile
inorganic aerosols**

V. A. Karydis et al.

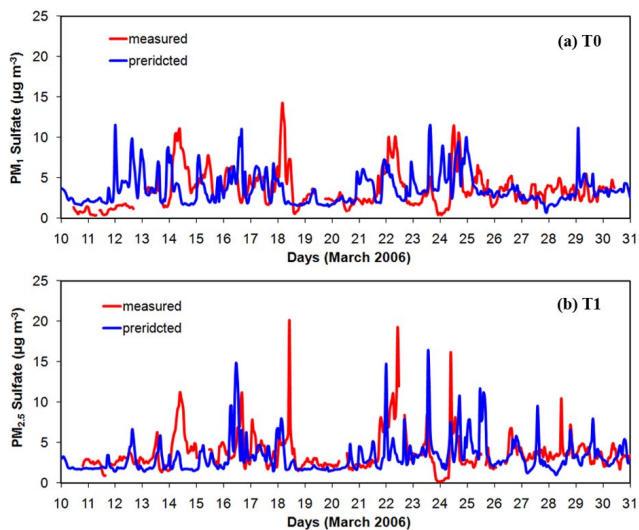


Fig. 4. Comparison of model hourly predictions against measurements for PM_{10} sulfate taken at T0 **(a)** and $\text{PM}_{2.5}$ sulfate taken at T1 **(b)**, during the MILAGRO campaign.

[Title Page](#)[Abstract](#)[Introduction](#)[Conclusions](#)[References](#)[Tables](#)[Figures](#)[◀](#)[▶](#)[◀](#)[▶](#)[Back](#)[Close](#)[Full Screen / Esc](#)[Printer-friendly Version](#)[Interactive Discussion](#)

Formation of semivolatile inorganic aerosols

V. A. Karydis et al.

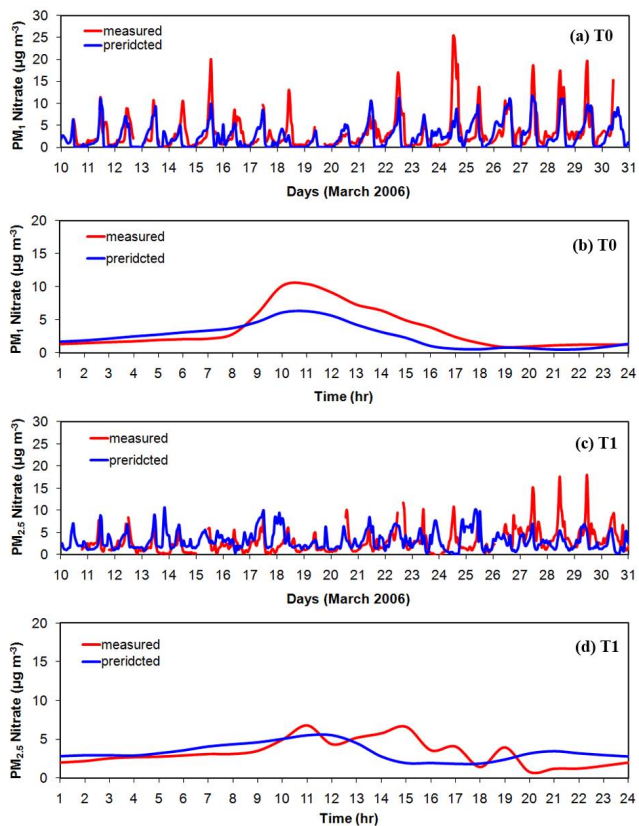


Fig. 5. Comparison of model hourly and diurnal predictions against measurements for PM_1 nitrate taken at T0 (a, b) and $\text{PM}_{2.5}$ nitrate taken at T1 (c, d) during the MILAGRO campaign.

Title Page

Abstract Introduction

Conclusions References

Tables Figures

◀ ▶

◀ ▶

Back Close

Full Screen / Esc

Printer-friendly Version

Interactive Discussion



**Formation of
semivolatile
inorganic aerosols**

V. A. Karydis et al.

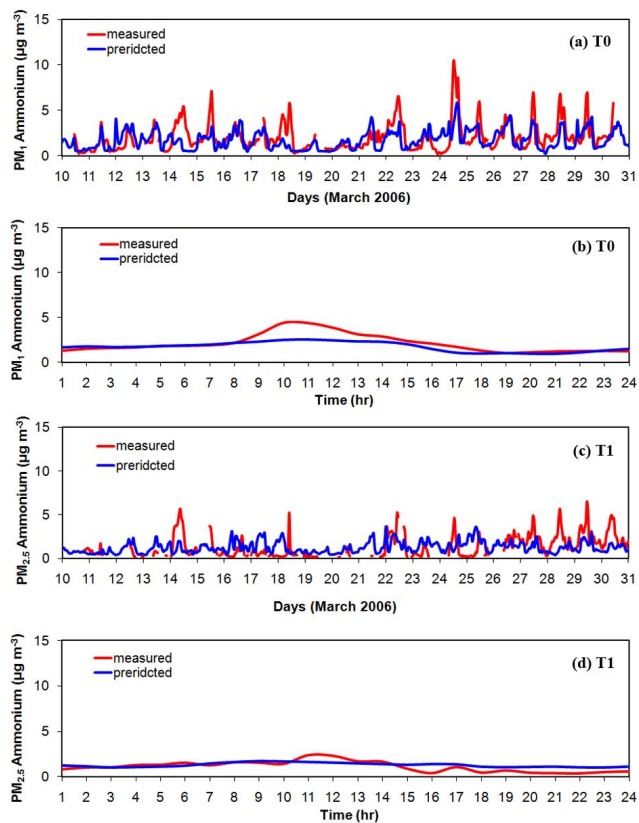


Fig. 6. Comparison of model hourly predictions against measurements for PM_1 ammonium taken at T0 (a, b) and $\text{PM}_{2.5}$ ammonium taken at T1 (c, d) during the MILAGRO campaign.

Formation of semivolatile inorganic aerosols

V. A. Karydis et al.

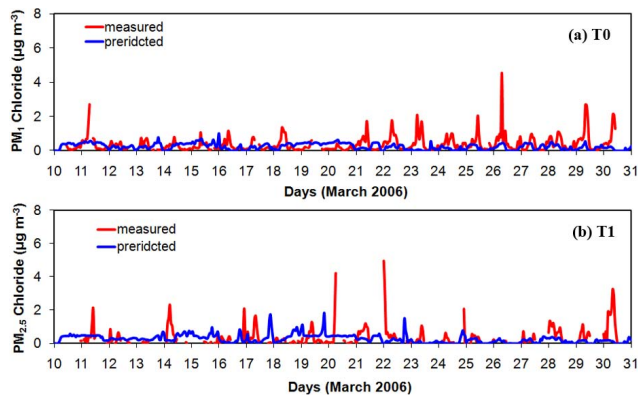


Fig. 7. Comparison of model hourly predictions against measurements for $\text{PM}_{1.0}$ chloride taken at T0 **(a)** and $\text{PM}_{2.5}$ chloride taken at T1 **(b)** during the MILAGRO campaign.

[Title Page](#)[Abstract](#)[Introduction](#)[Conclusions](#)[References](#)[Tables](#)[Figures](#)[◀](#)[▶](#)[◀](#)[▶](#)[Back](#)[Close](#)[Full Screen / Esc](#)[Printer-friendly Version](#)[Interactive Discussion](#)

**Formation of
semivolatile
inorganic aerosols**

V. A. Karydis et al.

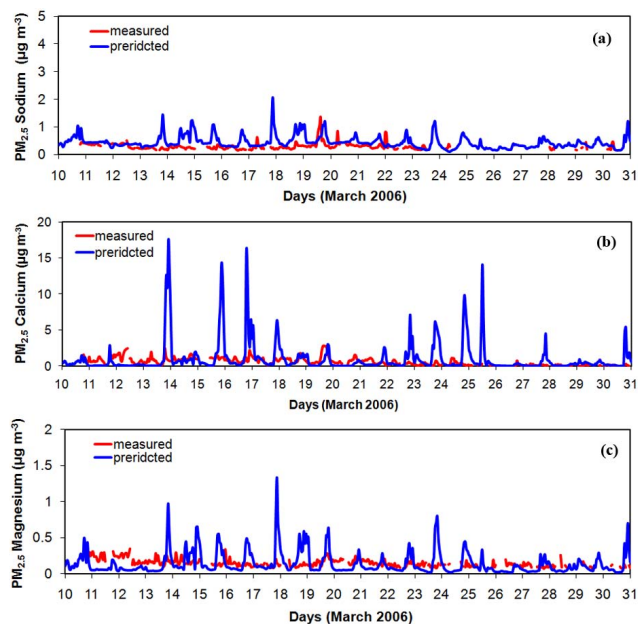


Fig. 8. Comparison of model hourly predictions against measurements for PM_{2.5} (a) sodium, (b) calcium, (c) magnesium taken at T1 during the MILAGRO campaign.

[Title Page](#)[Abstract](#)[Introduction](#)[Conclusions](#)[References](#)[Tables](#)[Figures](#)[◀](#)[▶](#)[◀](#)[▶](#)[Back](#)[Close](#)[Full Screen / Esc](#)[Printer-friendly Version](#)[Interactive Discussion](#)

Formation of semivolatile inorganic aerosols

V. A. Karydis et al.

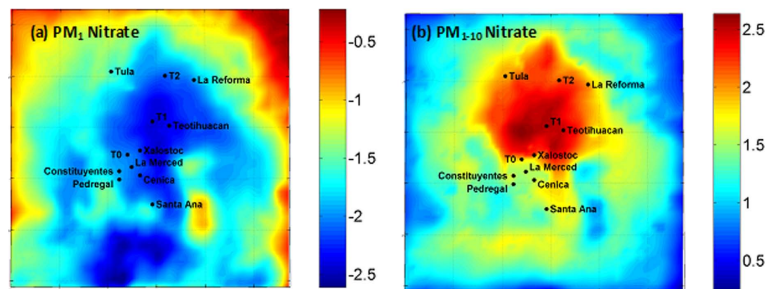


Fig. 9. Predicted change in ground-level concentrations ($\mu\text{g m}^{-3}$) of the **(a)** PM_1 nitrate and **(b)** PM_{1-10} nitrate after using the equilibrium approach for aerosol dynamics (instead of the hybrid approach used in the basecase simulations). A positive change corresponds to an increase due to the use of the hybrid approach.

Title Page

Abstract

Introduction

Conclusions

References

Tables

Figures

◀

▶

◀

▶

Back

Close

Full Screen / Esc

Printer-friendly Version

Interactive Discussion



Formation of semivolatile inorganic aerosols

V. A. Karydis et al.

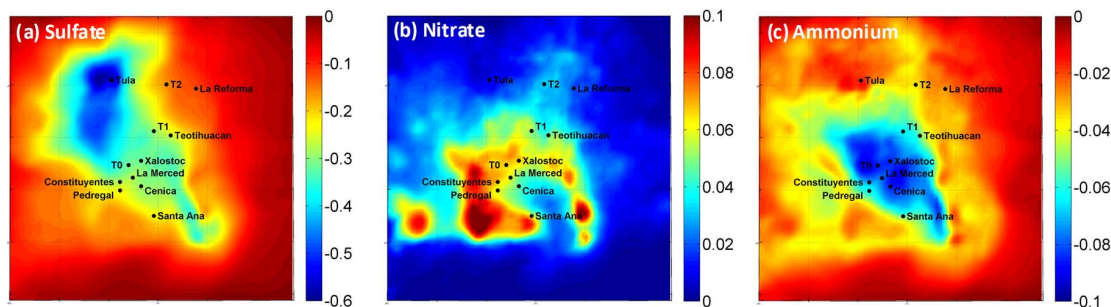


Fig. 10. Predicted change ($\mu\text{g m}^{-3}$) in ground-level concentrations of PM_{10} (a) sulfate, (b) nitrate, and (c) ammonium after a 50% reduction of SO_2 emissions. A negative change corresponds to a decrease.

Title Page

Abstract

Introduction

Conclusions

References

Tables

Figures

◀

▶

◀

▶

Back

Close

Full Screen / Esc

Printer-friendly Version

Interactive Discussion



**Formation of
semivolatile
inorganic aerosols**

V. A. Karydis et al.

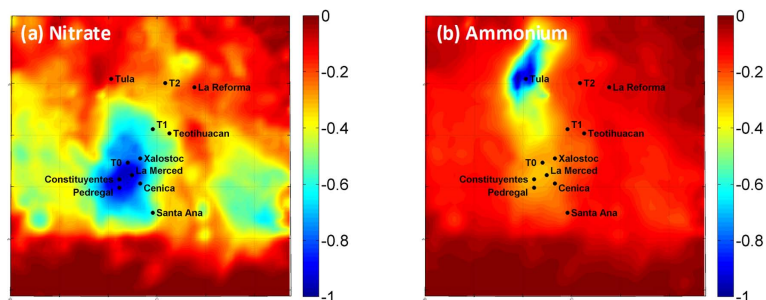


Fig. 11. Predicted change ($\mu\text{g m}^{-3}$) in ground-level concentrations of PM_{10} **(a)** nitrate, and **(b)** ammonium after a 50% reduction of NH_3 emissions. A negative change corresponds to a decrease.

Title Page

Abstract

Introduction

Conclusions

References

Tables

Figures

◀

▶

◀

▶

Back

Close

Full Screen / Esc

Printer-friendly Version

Interactive Discussion



Formation of semivolatile inorganic aerosols

V. A. Karydis et al.

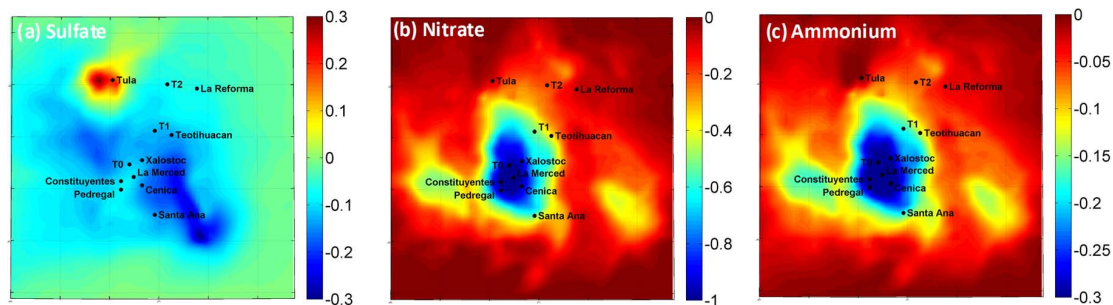


Fig. 12. Predicted change ($\mu\text{g m}^{-3}$) in ground-level concentrations of PM_{10} (a) sulfate, (b) nitrate, and (c) ammonium after a 50% reduction of NO_x emissions. A negative change corresponds to a decrease.

Title Page

Abstract

Introduction

Conclusions

References

Tables

Figures

◀

▶

◀

▶

Back

Close

Full Screen / Esc

Printer-friendly Version

Interactive Discussion

